HHS Public Access

Author manuscript

Min Metall Explor. Author manuscript; available in PMC 2023 May 11.

Published in final edited form as:

Min Metall Explor. 2022 February 12; 39(2): 241–249. doi:10.1007/s42461-022-00566-4.

A Comprehensive Roof Bolter Drilling Control Algorithm for Enhancing Energy Efficiency and Reducing Respirable Dust

H. Jiang[1], **Y. Luo**[2]

[1]National Institute for Occupational Safety and Health (NIOSH), Centers for Disease Control and Prevention, Pittsburgh, PA, USA

[2]Department of Mining Engineering, West Virginia University, Morgantown, WV, USA

Abstract

In underground coal mines, the drilling process in roof bolting operation could generate excessive amount of respirable coal and quartz dusts. Improper drilling control might also pose safety hazard and interrupt production. Therefore, an automated, high-efficiency drilling control system with safety features can be beneficial to the bolter personnel. In this research, a comprehensive drilling control algorithm has been developed to reduce the generation of respirable dust and to increase the drilling energy efficiency based on laboratory drilling test results and safety considerations. Specific energy is used to evaluate the energy efficiency. In addition, the ratio between specific energy and rock uniaxial compressive strength can be used as a basis for determining the rational drilling bite depth—typically a determined high one permissible by the driller power and drill steel. The test results show that to achieve and maintain a desired drilling bite depth for good drilling performance, a combination of relatively low rotational rate and a rationally high penetration is preferred. By monitoring the drilling rate, the system is able to evaluate the bit wear condition and improve drilling safety. In this paper, the developed drilling control algorithm for achieving a rational drilling bite depth is demonstrated. By adapting this drilling control algorithm, the drilling efficiency and bit condition can be monitored in real time, so the system can maintain a relatively high energy efficiency, generate less respirable dust, and avoid drilling failure.

Keywords

Roof bolter; Drilling control; Respirable dust; Specific energy; Bit condition

1 Introduction

Roof bolting is the most cost-effective and widely adapted application to improve mine safety by preventing roof falls for underground coal mines. However, the drilling process involved in the bolting operation can exposure a high concentration of respirable coal and

✉H. Jiang, hujiang@mix.wvu.edu.

Conflict of Interest The authors declare that there is no conflict of interest.

Disclaimer The findings and conclusions in this manuscript are those of the authors and do not necessarily represent the official position of the National Institute for Occupational Safety and Health (NIOSH), Centers for Disease Control and Prevention (CDC). Mention of company names or products does not constitute endorsement by NIOSH or CDC.

crystalline silica dusts (size < 10 μm) to the operator [1]. The negative health effect of coal and quartz particles in the respirable size range can increase dramatically because of the elevated chance for such particles to deposit in the alveolar region of lung. Working under overexposure environment can cause coal workers' pneumoconiosis (CWP), silicosis, and other chronic lung diseases; some of these illnesses are disabling, irreversible, and even fatal [2]. Overexposure of high-level quartz dust for a roof bolter operator can lead to development of silicosis in as little as 3 years [3]. Since quartz was commonly found from the roof strata, roof bolter drilling process could be the major quartz source for causing silicosis for bolter operators.

Investigations on the respirable coal and quartz dust hazards presented during underground roof bolting cycle were conducted by researchers [4]. The particle size distributions and quartz contents for 26 dust samples collected from different mine sites were analyzed. The results indicate a quartz content of more than 50% can be found from the total roof bolting dust. For the sub-5 μm fraction, the quartz content can be as much as 20%. These quantified results confirmed that roof bolting dust contains more percentage of quartz than other dust sources from mining activities.

Several dust control technologies, such as vacuum dust collection system and canopy air curtain, have been developed and implemented to address the exposure issue for roof bolter operator [5, 6]. However, new cases of CWP and silicosis were continued to be reported with a new younger-age trend. These can be caused by improved mining capability or new mining practices which elevated the generation of respirable coal and crystalline silica dust.

Based on the knowledge obtained from past research, the characteristics of respirable dust generation from drilling are not only rock property specific, but also drilling parameter specific [7, 8]. In this study, a drilling control algorithm is proposed, it is expected to reduce the generation of respirable dust while enhancing the energy efficiency. In addition, the drilling efficiency and bit condition can be evaluated while drilling based on the real-time feedback parameters. This capability enables the algorithm to ensure the drilling is performed under a relatively high energy efficiency with less respirable dust generation, and avoid drilling with excessive worn bit that can cause bit clogging or steel buckling failure.

2 Laboratory Drilling Experiments

In order to investigate the relationship between respirable dust generation with drilling parameters, including bit condition and rock type, 52 laboratory drilling tests have been conducted on a drilling test platform, shown in Fig. 1. This platform is equipped with a drilling control system, a data acquisition system, and a dust collection system. The drilling control system consists of the drill string and a control unit. This system attains the pre-set penetration and rotational rates for each drill hole event, which then automatically operates the drill to maintain the pre-set parameters. The data acquisition system obtains and records the drill bit position, penetration and rotational rates, drilling torque (T), thrust (W), etc. The dust collection system includes a pre-cleaner cyclone intended for rejecting non-airborne cutting particles, and a collection box that collects the remanent fine dusts in the air.

Since bolt-hole drilling in hard rock can produce more fine dust, faster bit wear, and unsafe working conditions than drilling in soft rocks, the drilling tests were performed on two rock blocks with different strengths. The uniaxial compressive strengths of the concrete and nonhomogeneous sandstone blocks are 55.16 and 132.13 MPa, respectively, to represent the medium and high strength rocks in the coal mine roof. The Kennametal® tungsten carbide spade bits, shown in Fig. 2, of 2.540 cm (1 inch) and 3.493 cm (1–3/8 inch) in diameter were used in the tests. For most of the tests, a new bit was used during drilling for each of the drill holes. For evaluating the effects of bit wear, a number of worn bits collected from the past drilling tests with varying weight losses were used in the tests, and a new bit was continuously used during drilling the holes until it was well worn.

The experiments were designed to drill the holes with a full range of bite depth according to the rock strengths, bit design, drilling safety, and available drilling power. The drilling system can be set at different penetration and rotation rates to achieve the pre-set bite depth for each test. The maximum allowable bite depth is limited by the available drilling thrust and the maximum allowable thrust on the drill steel to avoid it from bending failure [9–11]. In this study, drilling bite depth (b), defined as bit penetration depth per revolution, was introduced to describe the roof bolter drilling process. Drilling bite depth can be calculated from penetration (v) and rotational rate (w), expressed by Eq. (1).

$$b = \frac{60v}{w} \tag{1}$$

The detailed drilling parameters and conditions for the four groups are listed in Table 1. The first two groups were drilled with the larger bits (3.493 cm), while the smaller bits (2.540 cm) were used for groups 3 and 4. Test groups 1, 2, and 4 were conducted on concrete block, and group 3 was drilled on sandstone. It should be noted that for tests in group 1, a new bit was used for the first test and it was used continuously until it was substantially worn out after test 9. For tests 10, 11, and 12, three worn bits from past tests were used with a weight loss of 1.62 g (1%), 25.31 g (12%), and 27.54 g (13%), respectively.

Prior to creating each drill hole, the dust collection system was cleaned. After each drill test, dust samples from the stages of the dust collection system were collected and their weights were measured and recorded. A specified quantity of dust representing each bulk sample is taken by the coning and quartering method so that the size distribution for the entire sample could be accurately determined [12, 13]. The main drilling test parameters and dust generation results are also listed in Table 1. The implementation rate in the table indicates the ratio of the achieved bite depth to the pre-set bite depth. It should be noted that an implementation ratio significantly smaller than 100% reflects a poor bit condition or the limitation of available drilling power.

The specific energy is used for evaluating the energy efficiency in this study. This parameter is widely used in drilling research for the evaluation of the drilling condition and bit selection [14, 15]. The drilling specific energy is the amount of energy consumed to break a unit volume of rock, expressed in the amount of input energy divided by the rock volume drilled [16]. Therefore, according to its definition, specific energy can be used as a drilling

energy efficiency indicator, as higher specific energy means more energy was consumed during drilling of a unit volume of rock, indicating a lower energy efficiency. The specific energy for rotary drilling can be expressed mathematically in terms of drilling bite depth, penetration rate, torque, and thrust, as shown in Eq. (2) [17].

$$\varepsilon = \frac{2\pi T}{A_b \cdot b} + \frac{W}{A_b} \tag{2}$$

In the equation, A_b is the borehole area in cm^2, b is the drilling bite depth in cm/rev, and T and W are the torque and thrust in Nm and N, respectively. It should be noted that all these parameters were monitored and recorded in real time by the drilling control system.

3 Optimization of the Drilling Parameters

3.1 Rational Drilling Bite Depth Determination

The drilling inhalable and respirable dust weight, specific energy, and noise dose results were plotted against achieved bite depth in Fig. 3. It should be noted that only test results from 13 to 37 were included in this figure because these were all conducted with concrete block. For the noise dose data, these were obtained from a previous research project conducted under a same condition [18]. It was shown that specific energy reduced significantly while drilling with a larger bite depth, which also indicates a better energy efficiency with higher bite depth. Seventy percent reduction was achieved when increasing the bite depth from 0.152 to 0.732 cm/rev. The noise dose data show a rapid decrease as bite depth increases until bite depth reaches 0.541 cm/rev. After reaching the minimum value, no further remarkable decreases were found.

Both inhalable and respirable dust weight results show similar trends as noise dose data. Before bite depth reaches 0.551 cm/rev, dust generation decreases as the bite depth gets higher. However, after this point, the amount of inhalable dust becomes with further increase in bite depth. Meanwhile, the respirable dust shows an uptick after this operation point. Overall, the generated inhalable and respirable dust have reduced by 550 g and 200 g, respectively, within the tested drilling bite depth range.

This discussion reveals that drilling with a high bite depth has advantage in dust and noise control, as well as energy conservation. Since both dust and noise curves reach the turning point around a bite depth of 0.55 cm/rev and further reduction in energy efficiency is insignificant, the bite depth range of 0.50 to 0.60 cm/rev is recommended based on the particular condition for the purpose of dust reduction.

3.2 Drilling Performance Considerations

Drilling in different materials may encounter different operational and safety issues. Drilling hard materials normally requires a greater thrust, while an excessive thrust could bend the drill steel which can lead to its buckling failure and unsafe working environment. In addition, the excessive thrust, along with a high rotational rate, could accelerate the bit wear, which in turn prevents the bit from penetrating into the rock material but causing considerable rubbing action. When dealing with soft rocks with excessive bite depth, large

cuttings can be generated, and these cuttings could clog the drill bit and steel. The clogging could slow down the drilling cycle, and even worse, it can create a burst of dust backward out of the drilling hole. The dust burst exposes the operator to a high concentration of respirable dust and worsens the working environment.

The roof bolter drilling performance was analyzed using the field test data in four Central Appalachian coal mines with different roof conditions, as shown in Table 2 [19]. For each mine, two sets of drilling control parameters are listed. The upper row is the original operating parameter, while the lower row shows the adjusted parameter.

The frequency of clogging in drilling soft rocks in Mines A and C is significantly reduced after rationally increasing the bite depth. Drill stalling when drilling hard material in Mine A also was eliminated with lifted bite depth, and similar outcomes were shown from Mines C and D. Meanwhile, by applying a higher bite depth, bit life was extended significantly from the observations.

In addition, based on the soft material drilling performance from Mine A and C, it is found that reducing rotation rate is very effective in abating bit clogging problems. To avoid drill stalling, a higher penetration rate combined with a lower rotation rate is recommended, and performance improvements can be found from the tests in Mine C and D. To explain this phenomenon, a higher penetration rate with a lower rotational rate combination can achieve a higher cutting efficiency. Even though a higher penetration rate requires higher thrust input, the increase in effective thrust acting on rock reduces the thrust load on steel. Evidence of more efficient drilling in hard material can be found from the extended bit life in Mine D. Therefore, in order to provide a more efficient and safer drilling process, a higher torque and thrust combination is recommended to provide a rational high bite depth for the specific rock material.

4 Development of a Comprehensive Drilling Control Algorithm

Based on the results from the drilling energy and dust generation analysis, the rational drilling bite depth should be in the range from 0.50 to 0.60 cm/rev for the tested concrete blocks or rocks with similar strengths. For safe and smooth drilling performance, the rational strategy is finding a rational bite depth by reducing the rotation rate first and then increasing the penetration rate.

The rational bite depth range is dependent on the rock strength, bit design, and machine power. Uniaxial compressive strength (UCS) is a key physical parameter for estimating rock mass strength and is useful in determining the penetration rate in drilling performance prognosis across the drilling industry [20]. Therefore, it is good to develop a normalized specific energy against bite depth graph based on the UCS of the rock to be drilled as shown in Fig. 4. In this chart, both the vertical axis (specific energy) and the horizontal axis (bite depth) are normalized by UCS. This chart can be referred to when determining the rational drilling bite depth, which is the optimum bite depth when the other limitations are considered as the strength of rock strata changes.

In the chart in Fig. 4, the horizontal axis shows the UCS weighted drilling bite depth (b') defined by Eq. (3). It takes into account both the UCS of the tested concrete block and of the rock to be drilled. On the vertical axis, the UCS normalized specific energy shows the potential for further reduction in drilling specific energy caused by increased bite depth. The rational bite depth is determined when the reduction of specific energy is no longer significant, while the further increase in bite depth will be limited by drill steel safety, available drilling power (stalling), or clogging condition.

$$b' = b \cdot UCS_c / UCS_r \tag{3}$$

In Eq. (3), b' is the weighted drilling bite depth (cm/rev), UCS_c is the UCS for concrete block used in this test (MPa), and UCS_r is the UCS for the rock to be drilled (MPa).

The UCS normalized specific energy versus weighted bite depth from our drilling experiments shown in Fig. 3 can be well fitted with a negative power function. By substituting the ε and b' into the resulting regression equation in the figure, the relationship between ε, USC_r and b is expressed by Eq. (4). According to Eq. (2), ε could be affected by bit size, bit type, and drilling condition, so it should be noted that a drilling coefficient α needs to be applied in order to accurately calculate the ε when drilling under different conditions.

$$\varepsilon = 0.0444 \cdot \alpha \cdot UCS_r^{1.76528} \cdot b^{-0.76528} \tag{4}$$

As stated before, the optimum bite depth is the one when the specific energy reaches the minimum. However, it is impractical to achieve the optimum bite depth due to the safety and power limitations. A rational bite depth is that for which the further increase in bite depth will only result in an insignificant reduction in drilling specific energy. The rate of ε reduction is the first derivative of ε with respect to b (Eq. 5). The percent reduction in ε per 0.01 cm/rev bite depth increase is plotted in Fig. 4.

$$\frac{d\varepsilon}{db} = -0.03398 \cdot \alpha \cdot UCS_r^{1.76528} \cdot b^{-1.76528} \tag{5}$$

Figure 4 shows that as the bite depth increases, the specific energy decreases, indicating a better energy efficiency. The less specific energy means less energy is used for over-breaking the rock and for generating noise. According to analyses on the experiments for drilling dust and noise research on concrete blocks, the recommended bite depth range is between 0.5 and 0.6 cm/rev. The rate of ε reduction plotted in Fig. 2 also confirms that in the recommended rational bite depth range, the ε reduction per every 0.01 cm/rev bite depth increase is less than 1.5%. Therefore, the δ value is determined to be between 1.35 and 1.60. This range of δ value is applicable to all rock materials to be drilled other than wet and soft rocks with significant plastic behavior in which excessive bite depth can cause frequent clogging. A similar approach was used and proved to be effective in the optimization of the drilling

parameters for rotary downhole drilling [21]. Therefore, this ratio could provide an objective tool to determine whether the drilling was conducted in its rational performance range.

The recommended drilling control algorithm is shown in Fig. 5. In a real-time drilling process, the drilling parameters (i.e., penetration and rotational rates, thrust, and torque) acquired are used with bite design and wear condition to determine rock strengths. The rock strength is then used to determine the rational bite depth. Since a higher rotation rate (RPM) would accelerate bit wear, a lower RPM combined with a correlated penetration rate (ROP) is preferable to reach a targeted drilling bite depth. In addition, an excessively worn drill bit prevents the system in achieving the targeted bite depth and can increase the respirable and inhalable dust generation rate by as much as 61.5% (respirable) and 43.6% (inhalable). The overall drilling specific energy using a worn bit is higher than a new bit due to the increased rubbing area and friction between the drill bit and the rock. Therefore, a bit wear condition check is included in the algorithm according to the implementation rate (achieved versus targeted bite depth).

When the drill penetrates a different rock layer with its determined strength significantly different from the previous layer, a rational bite depth is determined based on the rock UCS and bit wear condition and implementation rate. As the drilling progresses, the specific energy is monitored, and the ratio can be calculated simultaneously. If the ratio is within 10% off the efficiency index, then the system will continue drilling with the initial bite depth. However, the algorithm still needs to evaluate the bit condition using the implementation rate. If the implementation rate is lower than the bit condition index, the system will stop, and a new bit needs to be installed to continue drilling.

If the ratio between specific energy and material UCS is higher than 110% δ when start drilling, the algorithm will reduce the rotational rate or increase the penetration rate to lift the bite depth in order to lower the specific energy to meet the criteria. However, if the system input increased to its cap power and the ratio is still off the range. This can indicate a low effective thrust, which was caused by excessive bit wear. Therefore, a bit replacement can be triggered to avoid steel buckling event.

By adapting this drilling control algorithm, the drilling efficiency and bit condition can be monitored in real time, so that at any point of the drilling, the system can stay in a relatively high energy efficiency with less respirable dust production and also reduce the chance to encounter bit clogging and steel buckling event, which can expose a tremendous safety and health hazard to the operator. Due to the limitation of data source, to improve the algorithm’s prediction accuracy for respirable dust and noise production rate, more dust and noise results from drilling different types of rock need to be collected for the calibration process.

5 Conclusions

Fifty-two laboratory drilling tests with two different bit sizes and rock types were conducted in this study. The particles generated from each drilling were sampled and analyzed. The energy input was analyzed for the efficiency evaluation and used to determine the optimal

drilling parameters. Regardless of bit size, on average, from one concrete drilling with a new bit, 20.9% of the total generated particles can be respirable and 56.5% can be inhalable. For sandstone drilling, the respirable and inhalable dust generation percentage is 20.9 and 74.4%, respectively.

By analyzing the effect of drilling bite depth on energy and dust generation rate, decreasing trends were observed for each parameter when increasing the bite depth. Based on the drilling safety performance, in order to provide a more efficient and safer drilling process, a higher torque and thrust combination to provide a rational high bite depth for the specific rock material are recommended.

An integrated drilling control algorithm was developed to improve the drilling efficiency and reduction of respirable dust. The ratio between specific energy and rock UCS was used as the index to identify rational drilling parameters for different materials.

This algorithm can monitor the drilling efficiency as well as the bit wear condition. Therefore, the algorithm can help to keep the drilling operation under a high efficiency while maintaining the dust generation rate at a lower level and reducing the chances of bit clogging and steel buckling events.

Acknowledgements

Data from this manuscript were presented at the 18th North American Mine Ventilation Symposium (NAMVS 2021), June 12–17, 2021.

References

1. Goodman GVR, Organiscak JA (2002) An evaluation of methods for controlling silica dust exposures on roof bolters. Trans Soc Min Metallurg 312:133–138
2. Liu T, Liu S (2020) The impacts of coal dust on miners' health: A review. Environ Res 190. 10.1016/j.envres.2020.109849
3. MSHA (2014) Exposure to coal mine dust containing quartz, health hazard information card HH-47. https://arlweb.msha.gov/s&hinfo/blacklung/HHazardCards/HHS47.pdf. Accessed 21 Feb 2022
4. Joy GJ, Beck TW, Listak JM (2010) Respirable quartz hazards associated with coal mine roof bolter dust. Proceedings of the 13th U.S./North American Mine Ventilation Symposium, pp. 59–64
5. Fletcher (2013) Maintaining the fletcher dry dust suppression system®. https://www.jhfletcher.com/_files/ugd/8e4feb_071b48343f244847a30794e030402638.pdf. Accessed 21 Feb 2022
6. Reed WR, Klima S, Shahan M, Ross GJH, Singh K, Cross R, Grounds T (2019) A field study of a roof bolter canopy air curtain (2nd generation) for respirable coal mine dust control. Int J Min Sci Technol. 10.1016/j.ijmst.2019.02.005
7. Jiang H, Luo Y, Yang J (2018) The mechanics of bolt drilling and theoretical analysis of drilling parameter effects on respirable dust generation. J Occup Environ Hyg 15(9):700–713 [PubMed: 30081754]
8. Jiang H, Fuo Y, McQuerrey J (2018) Experimental study on effects of drilling parameters on respirable dust production during roof bolting operations. J Occup Environ Hyg 15(2):143–151 [PubMed: 29157141]
9. Luo Y, Qiu B, Li MM (2013) Reducing drilling noise in roof bolting operation through rationalized drilling. 23rd World Mining Congress, Montreal, Canada
10. Zhang R, Liu J, Sa Z, Wang Z, Shouqing Lu, Wang C (2020) Experimental investigation on multi-fractal characteristics of acoustic emission of coal samples subjected to true triaxial loading-unloading. Fractals 28(5):2050092

11. Zhang R, Liu J, Sa Z, Wang Z, Lu S, Lv Z (2021) Fractal characteristics of acoustic emission of gas-bearing coal subjected to true triaxial loading. Measurement. 10.1016/j.measurement.2020.108349
12. Zhu Q (2014) Coal sampling and analysis standards. IEA Clean Coal Centre, London, United Kingdom
13. Cheng J, Zheng X, Luo W, Lei Y, Borowski M, Li X, Song W, Wang Z, Wang K (2020) A Compound Binder of Coal Dust Wetting and Suppression for Coal Pile. Process Saf Environ Prot 147:92–102
14. Farrelly M, Rabia H (1987) Bit Performance and Selection: A Novel Approach. Proceedings of the Society of Petroleum Engineers of AIME, pp. 987–996
15. Cheng J, Wang Y, Lei Y, Zheng X, Luo W, Song W, Wang Z, Han F (2020) Study on Coal Dust Crusting for Coal Pile Based on a Compound Binder. Powder Technol 376:149–166
16. Teale R (1964) The concept of specific energy in rock drilling. Int J Rock Mech Min Sci Geomech 2:57–73
17. Luo Y, Peng SS, Finfinger G, Wilson G (2004) A Mechanical Approach to Estimate Roof Strata Strength from Bolting Drilling Parameters. Paper presented at 2004 SME meeting, Feb. 23–25, 2004, Denver, CO, Pre-print No. 04–190
18. Li MM (2015) Development of drilling control technology to reduce drilling noise during roof bolting operations. Dissertation, West Virginia University
19. Cotton D, Burgess T, Martin T (2015) Optimizing Drilling Parameters for Improved Bolting Safety and Performance. 34th International Conference on Ground Control in Mining, WV, pp. 1–7
20. Gong Q (2006) Development of a rock mass characteristics model for TBM penetration rate prediction. Dissertation of Nanyang Technological University, Singapore
21. Chen X, Gao D, Guo B, Feng Y (2016) Real-time optimization of drilling parameters based on mechanical specific energy for rotating drilling with positive displacement motor in the hard formation. J Nat Gas Sci Eng 35:686–694

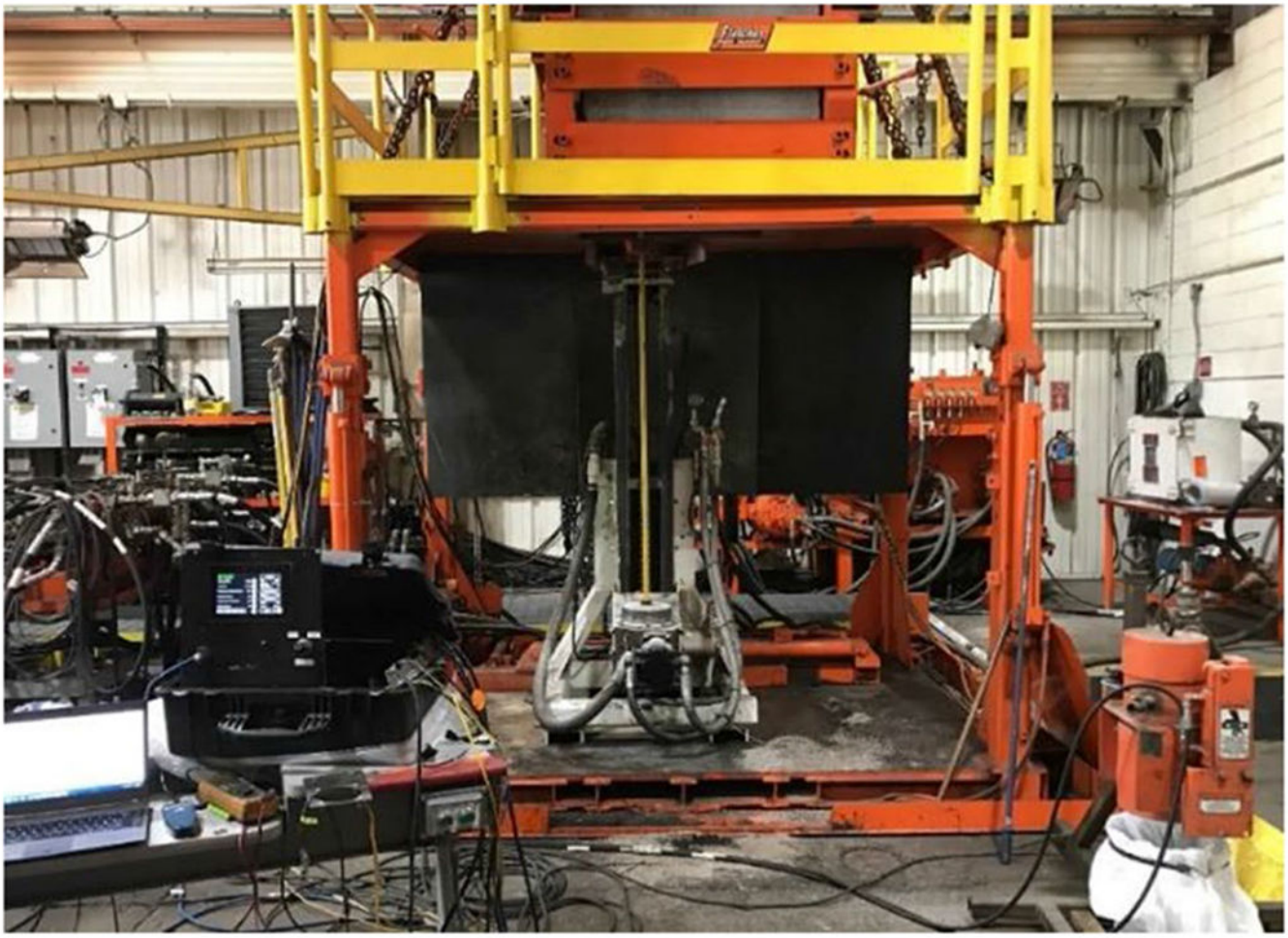

Fig. 1.
Fletcher® drilling test platform

Fig. 2.
The tungsten carbide spade bits with 1″ (left) and 1–3/8″ (right) diameter used

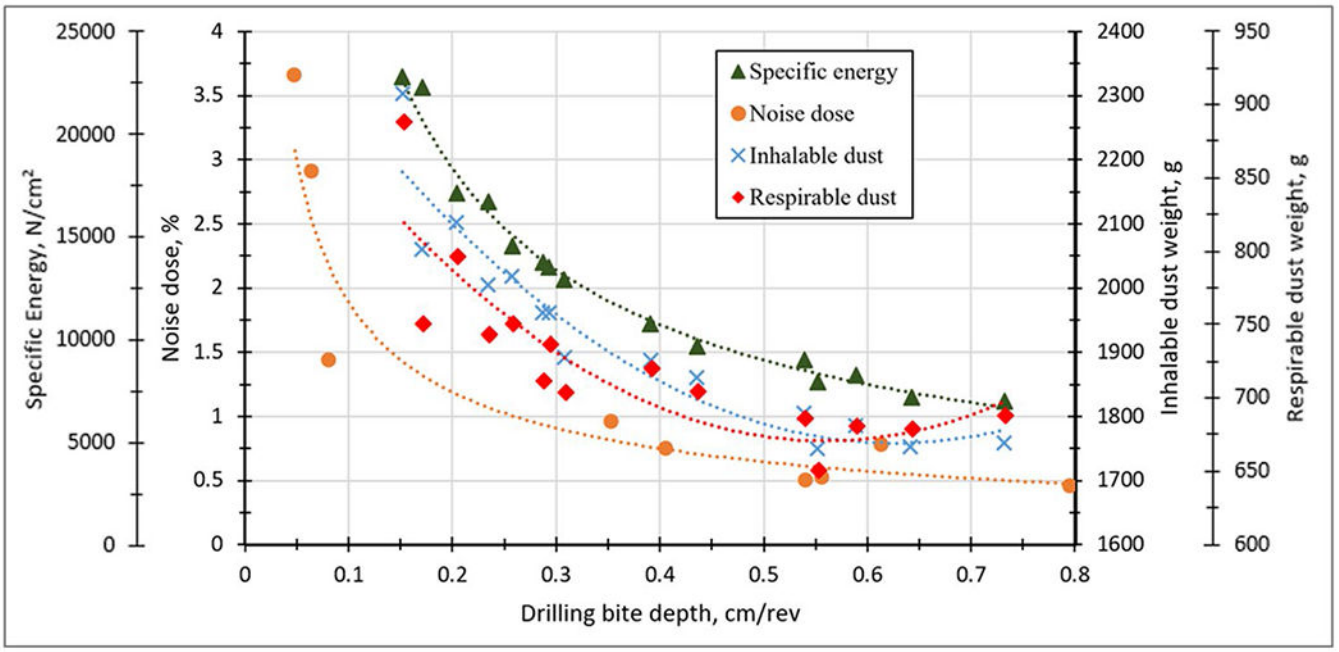

Fig. 3.

The relationship of drilling bite depth with noise dose, dust weight, and specific energy

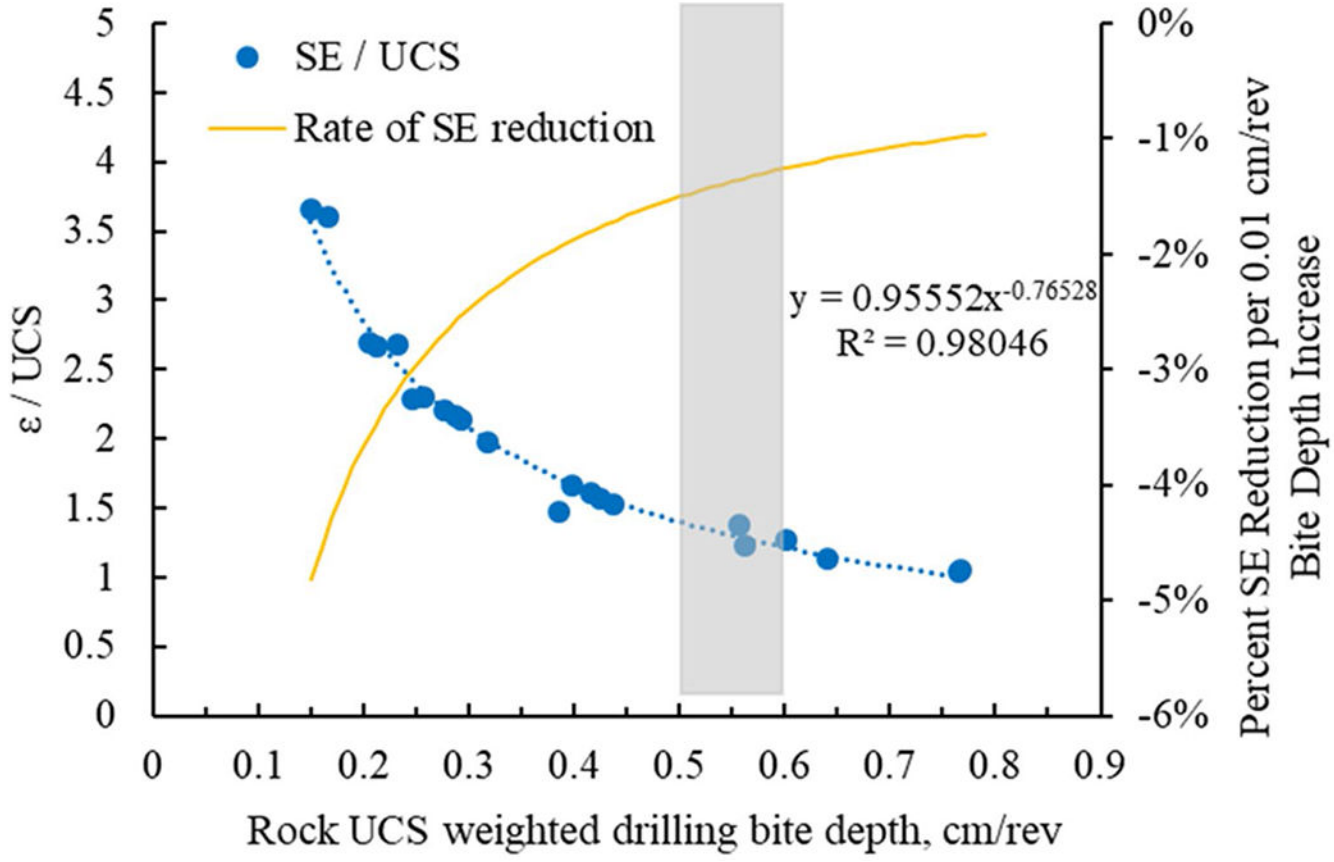

Fig. 4.
The relationship between weighted drilling bite depth with two different parameters

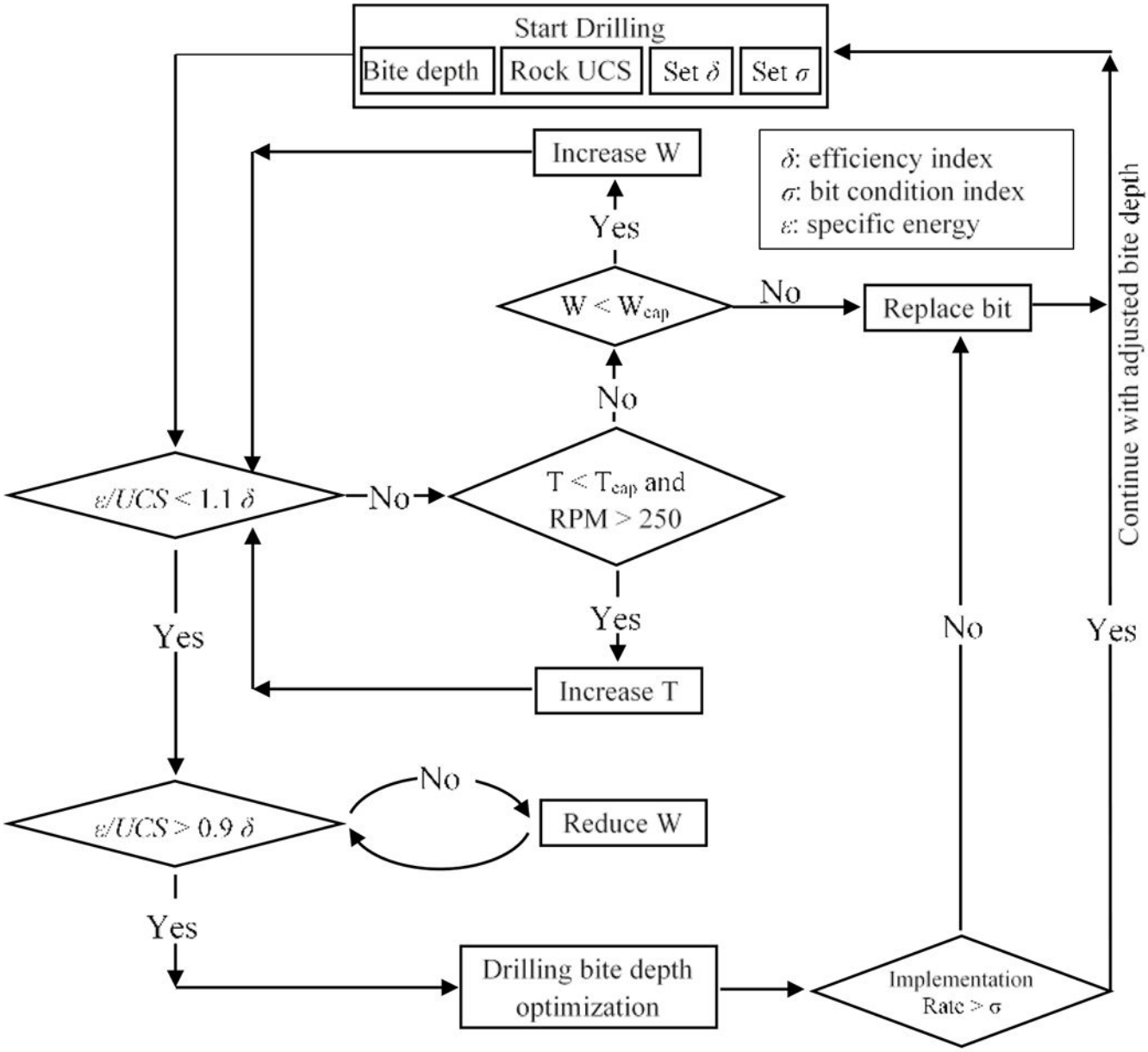

Fig. 5.
Schematic diagram of the drilling control algorithm

Min Metall Explor. Author manuscript; available in PMC 2023 May 11.

Table 1

Drilling parameters and feedback results for each drill hole*

Group	Test #	Condition	Pre-set	Achieved			Implem. Rate	Total inhalable dust	Total respirable dust	Specific energy
			b	*v*	*w*	*b*				
			cm/rev	*cm/s*	*rev/min*	*cm/rev*	*%*	*g*	*g*	*MPa*
1	1	Concrete; 1–3/8”	0.152	0.83	299	0.167	109.6	1803.3	757.3	248.0
	2		0.102	0.85	434	0.117	116.0	1953.0	757.8	414.7
	3		0.091	0.83	454	0.110	120.3	2136.1	837.7	443.0
	4		0.122	1.06	507	0.126	102.5	2207.4	925.8	420.6
	5		0.152	1.05	522	0.121	79.2	1995.0	803.6	467.4
	6		0.396	2.05	517	0.238	60.1	2293.0	910.4	249.2
	7		0.427	1.54	500	0.185	43.3	2297.3	856.2	300.8
	8		0.457	1.60	499	0.193	42.1	2032.6	804.2	276.1
	9		0.406	1.00	301	0.200	49.1	2430.9	1083.3	202.4
	10		0.213	1.71	497	0.206	96.6	1738.0	607.1	229.5
	11		0.213	1.31	497	0.158	74.0	2593.5	1126.1	333.0
	12		0.213	1.19	500	0.143	66.9	2670.5	1356.1	349.1
2	13	Concrete; 1–3/8”	0.122	1.15	462	0.150	122.0	2268.6	839.6	292.6
	14		0.152	1.09	392	0.167	109.0	2023.2	710.3	288.2
	15		0.183	1.61	470	0.205	112.7	2068.3	753.0	215.9
	16		0.213	1.78	502	0.213	99.6	1902.2	677.4	213.6
	17		0.218	1.58	409	0.232	106.7	1970.6	703.7	214.2
	18		0.244	2.06	503	0.246	100.9	1820.4	619.0	183.2
	19		0.244	2.14	500	0.257	105.4			190.8
	20		0.244	2.14	503	0.255	104.8			265.3
	21		0.244	2.11	491	0.257	105.8	1984.7	709.0	184.4
	22		0.274	2.32	501	0.277	101.1	1917.6	768.1	176.5
	23		0.274	2.40	501	0.287	104.6			167.8
	24		0.290	2.04	425	0.288	99.3	1927.2	672.6	173.2
	25		0.305	2.51	515	0.292	95.9	1930.2	696.5	171.3
	26		0.305	2.70	510	0.318	104.2	1859.7	665.7	158.3

Group	Test #	Condition	Pre-set	Achieved			Implem. Rate	Total inhalable dust	Total respirable dust	Specific energy
			b	*v*	*w*	*b*				
			cm/rev	*cm/s*	*rev/min*	*cm/rev*	*%*	*g*	*g*	*MPa*
	27		0.366	3.33	503	0.398	108.5	1857.5	681.9	133.4
	28		0.406	2.91	453	0.386	94.8	1648.5	648.1	117.6
	29		0.457	3.06	441	0.416	91.0	1651.8	558.0	129.2
	30		0.427	3.67	504	0.437	102.3	1830.1	666.9	121.8
	31		0.427	3.53	499	0.425	99.4	1742.7	672.8	125.8
	32		0.488	4.24	458	0.556	114.0	1775.7	649.8	110.6
	33		0.533	3.73	398	0.562	105.3	1719.8	616.3	98.0
	34		0.579	5.07	505	0.602	103.9	1757.6	645.3	101.6
	35		0.610	4.25	399	0.640	104.7	1724.2	644.7	90.5
	36		0.762	5.46	427	0.767	100.8	1730.9	653.2	84.0
	37		0.686	5.06	397	0.765	111.6	1785.7	656.7	83.2
3	38	Sandstone; 1–3/8”	0.305	1.67	485	0.206	67.8	365.9	97.4	282.0
	39		0.305	1.78	485	0.220	72.2	369.7	97.3	252.3
	40		0.305	2.05	488	0.252	82.7	354.8	96.5	223.8
	41		0.381	2.28	399	0.343	90.0	353.9	103.1	143.8
	42		0.610	3.14	482	0.391	64.1	362.7	100.6	154.5
	43		0.508	4.09	583	0.421	82.9	366.4	101.7	152.2
	44		0.508	4.16	574	0.434	85.6	364.2	98.4	144.6
	45		0.610	3.74	482	0.465	76.4	347.3	95.7	132.4
	46		0.762	3.20	387	0.496	65.1	675.4	200.9	120.1
	47		0.762	3.22	388	0.497	65.3	675.1	217.2	118.7
4	48	Concrete; 1”	0.127	1.20	591	0.121	95.7	1211.3	459.3	387.8
	49		0.416	3.68	554	0.399	96.0	1012.2	398.6	140.5
	50		0.416	3.86	553	0.418	100.7	987.6	374.8	136.1
	51		0.457	4.74	589	0.483	105.6	917.9	344.0	116.5
	52		0.572	3.99	391	0.611	107.0	1049.9	441.8	82.6

* Drilling tests 19, 20, and 23 encountered the steel rope imbedded in the reinforced concrete block; no dust sample was collected

Min Metall Explor. Author manuscript; available in PMC 2023 May 11.

Table 2

Roof bolter drilling performance in different roof conditions

	Strata	Rotation rate, rpm	Penetration rate, cm/s	*b*, cm/rev	Clogging	Stalling	Bit life, cm/bit
Mine A	29% soft shale	645	4.32 soft	0.402	Always	Sometimes	251
	71% hard shale		2.03 hard	0.189			
		487	4.45 soft	0.548	Rarely	Never	315
			4.06 hard	0.500			
Mine B	Medium hard	580	5.08	0.526	Never	Never	1 row/bit
		475	4.45	0.562	Never	Never	3 row/bit
Mine C	42% soft shale	670	6.10	0.546	Frequently	Frequently	1585
	58% med. hard	500	6.10	0.732	Rarely	Rarely	1585
Mine D	Extremely hard material	650	3.30	0.305	Rarely	Always	91
		650	4.06	0.375	Never	Rarely	366

*Frequency expressions for clogging and stalling event from high to low: Always, frequently, sometimes, rarely, never